



# On the MHD flow and heat transfer of a micropolar fluid in a rectangular duct under the effects of the induced magnetic field and slip boundary conditions

Hassan Nasr Ahamed Ismail<sup>1</sup> · Aly Maher Abourabia<sup>2</sup> · D. A. Hammad<sup>1</sup> · Nasrelden A. Ahmed<sup>1</sup> · A. A. El Desouky<sup>1</sup>

Received: 27 September 2019 / Accepted: 31 October 2019  
© Springer Nature Switzerland AG 2019

## Abstract

The heat and mass transfer due to the steady laminar and incompressible micropolar fluid flow through a rectangular duct with the slip flow and convective boundary conditions are numerically calculated. The fluid moves under an external magnetic field applied on a plane perpendicular to the axis of the duct. The governing nonlinear partial differential equations of momentum, microrotation, induction, and the energy are solved simultaneously by the finite difference method. The effect of various numbers and parameters such as Reynolds, magnetic Reynolds, Hartmann, coupling, Brinkman numbers, the slip flow and convective parameters are presented in graphs. Some comparisons with previous works are included.

**Keywords** Magnetohydrodynamics · Heat transfer · Micropolar fluid · Slip flow · Convection · Rectangular duct

## 1 Introduction

In the last years, several investigators have studied the fluid flow and heat transfer inside a rectangular duct which has received considerable attention in engineering applications. This type of fluid flow is observed in several mechanical types of the equipment and the heat exchangers. Eringen [1–3] studied the theory of generalized continuum configuration of micropolar fluids which exhibit the microrotational effects and microrotational inertia. Subba et al. [4] studied the nonsimilar boundary-layer solutions for mixed convective micropolar fluid flow around a rotating cone, they provided the microrotation boundary conditions and their influence on the gyration, velocity, and heat transfer fields. Vantighem [5] used the numerical simulation for steady flows of both laminar and turbulent in the quasi-static MHD flow through a toroidal

duct of square cross-section with insulating Hartmann and conducting sidewalls, they presented a comprehensive analysis of the secondary flow and a comparison between MHD and hydrodynamic flows. Chou et al. [6] used the numerical solutions for combined free and forced laminar convection through a horizontal rectangular duct by a vorticity-velocity method, the walls are heated with a uniform heat flux without the assumptions of the small Grashof number and large Prandtl number. The numerical study of Aung et al. [7] made a combination between the free and forced laminar convection through vertical parallel plates with asymmetric wall heating at the uniform heat flux (UHF). Mahaney et al. [8] used a numerical technique to solve the momentum and energy equations and studied the effects of buoyancy-induced secondary fluid flow on forced flow with uniform bottom heating through a horizontal rectangular duct. Huang et al. [9] investigated

✉ A. A. El Desouky, ahmed.mohammed@bhit.bu.edu.eg; Hassan Nasr Ahamed Ismail, hassan.ismaeel@bhit.bu.edu.eg; Aly Maher Abourabia, aly.abourabia@science.menofia.edu.eg; D. A. Hammad, doaa.hammad@bhit.bu.edu.eg; Nasrelden A. Ahmed, Nasereldein.ahmed@bhit.bu.edu.eg | <sup>1</sup>Basic Engineering Sciences Department, Benha Faculty of Engineering, Benha University, Benha 13512, Egypt. <sup>2</sup>Mathematics Department, Faculty of Science, Menoufia University, Shebeen Elkom 32511, Egypt.



numerically the mixed convection heat and mass transfer with film evaporation and condensation along the wetted wall with different temperatures and aspect ratios through the vertical ducts. Sayed et al. [10] investigated the laminar fully developed MHD flow and heat transfer of a viscous incompressible electrically conducting of a Bingham fluid in a rectangular duct, they took into consideration the constant pressure gradient, external uniform magnetic field and Hall effect. Rarnakrishna et al. [11] investigated the laminar natural convection of air for constant temperature and constant heat flux through a vertical square duct opened at both ends, they assumed that the velocity of air entering at the bottom of the duct is uniform at atmospheric pressure. Abd-Alla et al. [12] studied numerically the effect of magnetic field, rotation and initial stress on the motion of a micropolar fluid through a circular cylindrical flexible tube with small values of amplitude ratio, they considered that the wall properties is elastic or viscoelastic. Srnivasacharya et al. [13] investigated the steady flow of an incompressible and electrically conducting micropolar fluid flow with Hall and ionic effects in a rectangular duct, the government partial differential equations are solved numerically by the finite difference method. Pandey et al. [14] studied analytically the MHD flow of a micropolar fluid through a porous medium by sinusoidal peristaltic waves moving down the channel walls, the low Reynolds number and long wavelength approximations are applied to solve the nonlinear problem. Janardhana et al. [15] investigated numerically the thermal radiation heat transfer effect on the unsteady MHD flow of micropolar fluid over a uniformly heated vertical hollow cylinder using Bejan's heat function concept. Ayano et al. [16] investigated numerically of mixed convection flow through a rectangular duct under the transversely applied magnetic field with at least one of the sidewalls of the duct being isothermal, the governing differential equations have been transformed into a system of nondimensional differential equations and are solved numerically such as the velocity, temperature, and microrotation component profiles are displayed graphically. Miroshnichenko et al. [17] investigated numerically the laminar mixed convection of micropolar fluid through a horizontal wavy channel by the finite difference method, they solved the system of equations of dimensionless stream function, vorticity and temperature then, studied the effects of Reynolds, Rayleigh, Prandtl numbers, vortex viscosity parameter and undulation number onto streamlines, isotherms, vorticity isolines as well as horizontal velocity and temperature profiles. Shit et al. [18] investigated the effect of the slip velocity on the peristaltic transport of a physiological fluid through a porous non-uniform channel under low-Reynolds number and long wavelength, the flow characteristics of incompressible, viscous, electrically conducting micropolar fluid has been

derived analytically. Bhattacharyya et al. [19] investigated the combined influence between magnetic field and its dissipation on convective heat and mass transfer of a viscous chemically reacting fluid in the concentric cylindrical annulus, the inner cylinder is maintained at constant temperature and concentration while, the outer cylinder is maintained under constant heat flux. Sheremet et al. [20] investigated numerically the natural convection of a micropolar fluid in the triangular cavity, the system of micropolar equations of dimensionless stream function, vorticity and temperature have been solved by the finite difference method of the second-order accuracy under the initial and boundary conditions. Gupta et al. [21] studied numerically for the steady mixed convection (MHD) flow of micropolar fluid over a porous shrinking sheet, they assumed that the magnetic field and velocity of shrinking sheet are varied as a power functions of the distance from the origin. All the above studies are on the fluid flow and heat transfer under the magnetic field effect.

Our effort in this paper is dedicated to study the behavior of the micropolar fluid under the effect of *induced magnetic fields*. The micropolar fluid is flowing through a rectangular duct subjected to an applied magnetic field with the inclusion of both the effects of the induced magnetic field and the slip conditions.

## 2 The physical problem and mathematical modeling

Consider the steady laminar and incompressible flow of an electrically conducting micropolar fluid moving through a rectangular duct at a constant pressure gradient  $\partial P / \partial Z$  under transverse external magnetic flux density  $B_0$  applied in the X-direction. The fluid flow is generated due to the pressure gradient along the Z-direction of the duct. Choosing the coordinate system along the Z-axis to be the length of the duct and (X and Y) axis to be the cross-sectional area of the duct, as in Fig. 1. Each wall of the duct is kept at a uniform temperature ( $T_w$ ). Assume that the slip flow condition for the velocity in the walls is parallel to X-axis and the slip convective conditions are applied to the walls,

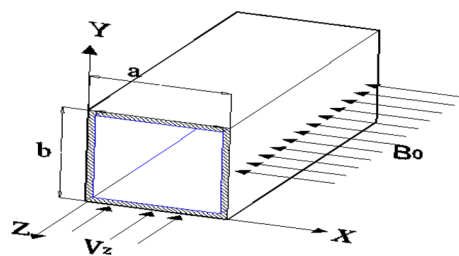


Fig. 1 Geometrical model of the duct flow

which is parallel to Y-axis. Assuming that the velocity vector of the micropolar fluid is  $\vec{V} = V_z(X, Y)\vec{k}$  and the micro-rotation vector  $\vec{\omega} = \omega_x(X, Y)\vec{i} + \omega_y(X, Y)\vec{j}$ . The fluid has a large magnetic Reynolds number ( $R_m$ ) so that the induced magnetic field is produced significantly inside the fluid.

#### The governing equations

The governing equations in a dimension of the flow of an incompressible and electrically conducting micropolar fluid [2] with the induced magnetic field and without of body force and body couple are

#### Continuity equation

$$\frac{\partial \rho}{\partial t} + \nabla \cdot (\rho \vec{V}) = 0 \quad (1)$$

$$\frac{\partial \vec{B}}{\partial t} = \nabla \times (\vec{V} \times \vec{B}) + \frac{1}{\sigma \mu_m} \nabla^2 \vec{B}, \quad \vec{J} = \sigma (\vec{E} + \vec{V} \times \vec{B}), \quad \nabla \cdot \vec{E} = 0, \quad \nabla \times \vec{B} = \mu_m \vec{J}, \quad \nabla \times \vec{E} = \frac{\partial \vec{B}}{\partial t}, \quad \nabla \cdot \vec{B} = 0 \quad (6)$$

#### Momentum equation

$$\rho \frac{D\vec{V}}{Dt} = -\nabla P - (\mu + k) \nabla \times \nabla \times \vec{V} + k \nabla \times \vec{\omega} + \vec{J} \times \vec{B} \quad (2)$$

#### Microrotation equation

$$\rho j^* \frac{D\vec{\omega}}{Dt} = k \nabla \times \vec{V} - 2k \vec{\omega} - \gamma \nabla \times \nabla \times \vec{\omega} + (\tilde{\alpha} + \beta + \gamma) \nabla (\nabla \cdot \vec{\omega}) \quad (3)$$

#### Energy equation

$$\rho C_p \frac{DT}{Dt} = K_f \nabla^2 T + \lambda (\nabla \cdot \vec{V})^2 + 2\mu (D : D) + 4k \left( \frac{1}{2} \nabla \times \vec{V} - \vec{\omega} \right)^2 + \tilde{\alpha} (\nabla \cdot \vec{\omega})^2 + \gamma (\nabla \vec{\omega}) : (\nabla \vec{\omega}) + \beta (\nabla \vec{\omega}) : (\nabla \vec{\omega})^T + \frac{\vec{J}^2}{\sigma} \quad (4)$$

where  $\rho$ ,  $P$  and  $T$  are the fluid density, fluid pressure and temperature, respectively with  $j^*$ ,  $K_f$ ,  $C_p$ ,  $\sigma$  are the microgyration parameter, thermal conductivity, specific heat at constant pressure and the electrical conductivity,

respectively, while  $D$  is the deformation tensor ( $D = 0.5 (\vec{V}_{ij} + \vec{V}_{ji})$ ),  $\vec{J}$  is the electric current density vector,  $\vec{B}$  is the total magnetic field  $\vec{B} = (B_0 \vec{i} + B_{z(X,Y)} \vec{k})$  and  $B_z$  is the induced magnetic field and  $\mu$ ,  $k$ ,  $\tilde{\alpha}$ ,  $\beta$  and  $\gamma$  are the material constants (viscosity coefficients) which are satisfying the following inequalities;

$$k \geq 0, \quad 2\mu + k \geq 0, \quad 3\tilde{\alpha} + \beta + \gamma \geq 0, \quad \gamma \geq |\beta| \quad (5)$$

The induction equation, Ohm's law and Maxwell's equations related to the magnetic field  $\vec{B}$ , electric current density  $\vec{J}$  and electric field density vector  $\vec{E}$  are given by;

where  $\mu_m$  is the magnetic permeability. Due to that the system does not apply polarization voltage (each wall is an electrical insulator), the electric field density vector  $\vec{E}$  is neglected. Under the above assumptions, the MHD equations become

#### Induction equation

$$B_0 \left[ \frac{\partial V_z}{\partial X} \right] + \frac{1}{\sigma \mu_m} \left[ \frac{\partial^2 B_z}{\partial X^2} + \frac{\partial^2 B_z}{\partial Y^2} \right] = 0, \quad (7)$$

#### Momentum equation

$$-\left[ \frac{\partial P}{\partial Z} \right] + (\mu + k) \left[ \frac{\partial^2 V_z}{\partial X^2} + \frac{\partial^2 V_z}{\partial Y^2} \right] + k \left[ \frac{\partial \omega_y}{\partial X} - \frac{\partial \omega_x}{\partial Y} \right] + \frac{B_0}{\mu_m} \left[ \frac{\partial B_z}{\partial X} \right] = 0, \quad (8)$$

#### Microrotation equation in X-direction

$$-2k\omega_x + k \left[ \frac{\partial V_z}{\partial Y} \right] - \gamma \frac{\partial}{\partial Y} \left[ \frac{\partial \omega_y}{\partial X} - \frac{\partial \omega_x}{\partial Y} \right] + (\tilde{\alpha} + \beta + \gamma) \frac{\partial}{\partial X} \left[ \frac{\partial \omega_x}{\partial X} + \frac{\partial \omega_y}{\partial Y} \right] = 0, \quad (9)$$

#### Microrotation equation in Y-direction

$$-2k\omega_y - k \left[ \frac{\partial V_z}{\partial X} \right] + \gamma \frac{\partial}{\partial X} \left[ \frac{\partial \omega_y}{\partial X} - \frac{\partial \omega_x}{\partial Y} \right] + (\tilde{\alpha} + \beta + \gamma) \frac{\partial}{\partial Y} \left[ \frac{\partial \omega_x}{\partial X} + \frac{\partial \omega_y}{\partial Y} \right] = 0, \quad (10)$$

## Energy equation

where  $T_f$  is the initial temperature of the fluid, while  $\alpha^*$ 

$$\begin{aligned}
& k_f \left[ \frac{\partial^2 T}{\partial X^2} + \frac{\partial^2 T}{\partial Y^2} \right] + (\mu + k) \left[ \left( \frac{\partial V_z}{\partial X} \right)^2 + \left( \frac{\partial V_z}{\partial Y} \right)^2 \right] + \tilde{\alpha} \left[ \frac{\partial \omega_x}{\partial X} + \frac{\partial \omega_y}{\partial Y} \right]^2 + 2k \left[ \omega_x^2 + \omega_y^2 - \omega_x \frac{\partial V_z}{\partial Y} + \omega_y \frac{\partial V_z}{\partial X} \right] \\
& + \gamma \left[ \left( \frac{\partial \omega_x}{\partial X} \right)^2 + \left( \frac{\partial \omega_x}{\partial Y} \right)^2 + \left( \frac{\partial \omega_y}{\partial X} \right)^2 + \left( \frac{\partial \omega_y}{\partial Y} \right)^2 \right] + \beta \left[ \left( \frac{\partial \omega_x}{\partial X} \right)^2 + \left( \frac{\partial \omega_y}{\partial Y} \right)^2 + 2 \left( \frac{\partial \omega_x}{\partial Y} \frac{\partial \omega_y}{\partial X} \right) \right] \\
& + \frac{1}{\sigma \mu_m^2} \left( \frac{\partial^2 B_z}{\partial X^2} + \frac{\partial^2 B_z}{\partial Y^2} \right) = 0.
\end{aligned} \quad (11)$$

The boundary conditions are classified as follows [22];

$$B = 0, \quad V_z = 0, \quad \omega_x = 0, \quad \omega_y = 0 \quad \text{at} \quad X = 0 \quad \text{and} \quad X = a; \quad (12a)$$

$$k_f \frac{dT}{dX} - h(T - T_f) = 0 \quad \text{at} \quad X = 0; \quad (12b)$$

$$k_f \frac{dT}{dX} + h(T - T_w) = 0 \quad \text{at} \quad X = a; \quad (12c)$$

$$B = 0, \quad T = T_w, \quad \omega_x = 0, \quad \omega_y = 0, \quad \text{at} \quad Y = 0 \quad \text{and} \quad Y = b; \quad (12d)$$

$$V_z = \alpha^* \frac{dV_z}{dY} \quad \text{at} \quad Y = 0; \quad (12e)$$

and  $h$  are the slip flow coefficient and the slip convection coefficient, respectively. The dimensionless variables are introduced as follows;

$$\begin{aligned}
x &= \frac{X}{a}, \quad y = \frac{Y}{a}, \quad v = \frac{V_z}{V_0}, \quad \omega_1 = \frac{\omega_x a}{V_0}, \\
\omega_2 &= \frac{\omega_y a}{V_0}, \quad \theta = \frac{T - T_w}{T_f - T_w}, \quad B = \frac{B_z}{B_0}, \\
\frac{\partial P}{\partial Z} &= -\frac{\rho V_0^2}{a} P_l.
\end{aligned} \quad (13)$$

Substituting the Eqs. (13) into Eqs. (7)–(11), we get;

$$\left[ \frac{\partial v}{\partial x} \right] + \frac{1}{R_m} \left[ \frac{\partial^2 B}{\partial x^2} + \frac{\partial^2 B}{\partial y^2} \right] = 0 \quad (14)$$

$$R_e P_l + \left( \frac{1}{1-N} \right) \left[ \frac{\partial^2 v}{\partial x^2} + \frac{\partial^2 v}{\partial y^2} \right] + \left( \frac{N}{1-N} \right) \left[ \frac{\partial \omega_2}{\partial x} - \frac{\partial \omega_1}{\partial y} \right] + \frac{Ha^2}{R_m} \left[ \frac{\partial B}{\partial x} \right] = 0 \quad (15)$$

$$-\omega_1 + \left( \frac{1}{2} \right) \left[ \frac{\partial v}{\partial y} \right] + \left( \frac{2-N}{2m^2} \right) \left[ \frac{\partial^2 \omega_1}{\partial y^2} \right] + \left( \frac{1}{l^2} \right) \left[ \frac{\partial^2 \omega_1}{\partial x^2} \right] + \left( \frac{2m^2 - l^2(2-N)}{2m^2 l^2} \right) \left[ \frac{\partial^2 \omega_2}{\partial x \partial y} \right] = 0 \quad (16)$$

$$-\omega_2 - \left( \frac{1}{2} \right) \left[ \frac{\partial v}{\partial x} \right] + \left( \frac{2-N}{2m^2} \right) \left[ \frac{\partial^2 \omega_2}{\partial x^2} \right] + \left( \frac{1}{l^2} \right) \left[ \frac{\partial^2 \omega_2}{\partial y^2} \right] + \left( \frac{2m^2 - l^2(2-N)}{2m^2 l^2} \right) \left[ \frac{\partial^2 \omega_1}{\partial x \partial y} \right] = 0 \quad (17)$$

$$\begin{aligned}
& \left[ \frac{\partial^2 \theta}{\partial x^2} + \frac{\partial^2 \theta}{\partial y^2} \right] + Br \left[ \left( \frac{1}{1-N} \right) \left[ \left( \frac{\partial v}{\partial x} \right)^2 + \left( \frac{\partial v}{\partial y} \right)^2 \right] + \left( \frac{2N}{1-N} \right) \left[ \omega_1^2 + \omega_2^2 - \omega_1 \frac{\partial v}{\partial y} + \omega_2 \frac{\partial v}{\partial x} \right] \right. \\
& + A \left[ \frac{\partial \omega_1}{\partial x} + \frac{\partial \omega_2}{\partial y} \right]^2 + \left( \frac{N(2-N)}{m^2(1-N)} \right) \left[ \left( \frac{\partial \omega_1}{\partial x} \right)^2 + \left( \frac{\partial \omega_1}{\partial y} \right)^2 + \left( \frac{\partial \omega_2}{\partial x} \right)^2 + \left( \frac{\partial \omega_2}{\partial y} \right)^2 \right] \\
& \left. + C \left[ \left( \frac{\partial \omega_1}{\partial x} \right)^2 + \left( \frac{\partial \omega_2}{\partial y} \right)^2 + 2 \left( \frac{\partial \omega_1}{\partial y} \frac{\partial \omega_2}{\partial x} \right) \right] \right] + \frac{Ha^2 Br}{R_m^2} \left( \frac{\partial^2 B}{\partial x^2} + \frac{\partial^2 B}{\partial y^2} \right) = 0
\end{aligned} \quad (18)$$

$$V_z = \alpha^* \frac{dV_z}{dY} \quad \text{at} \quad Y = b; \quad (12f)$$

where  $m^2 = \frac{a^2 k(2\mu+k)}{\gamma(\mu+k)}$ ,  $A = \frac{\tilde{\alpha}}{\mu a^2}$  and  $C = \frac{\beta}{\mu a^2}$  are the micropolar parameters,  $N = \frac{k}{\mu+k}$  is the coupling number,  $l^2 = \frac{2a^2 k}{\tilde{\alpha} + \beta + \gamma}$

is dimensionless parameter,  $R_e = \rho V_0 a / \mu$  is the Reynolds number,  $R_m = \sigma \mu_m V_0 a$  is the magnetic Reynolds number,  $Ha = B_0 a \sqrt{\sigma / \mu} = \sqrt{R_e R_m} / Al$  is the Hartmann number,  $Al = V_0 / \sqrt{B_0^2 / \mu_m \rho}$  is the Alfven number,  $Br = \frac{\mu V_0^2}{k_f (T_f - T_w)}$  is the Brinkman number and the inverted pressure gradient  $P_I = 1 / \left( \frac{\partial P}{\partial z} \right)$ .

The boundary conditions in dimensionless form are.

$$B = 0, \quad v = 0, \quad \omega_1 = 0, \quad \omega_2 = 0 \quad \text{at} \quad x = 0 \quad \text{and} \quad x = 1; \quad (19a)$$

$$\frac{d\theta}{dX} - Bi(\theta - 1) = 0 \quad \text{at} \quad x = 0; \quad (19b)$$

$$\frac{d\theta}{dX} - Bi\theta = 0 \quad \text{at} \quad x = 1; \quad (19c)$$

$$B = 0, \quad \theta = 0, \quad \omega_1 = 0, \quad \omega_2 = 0, \quad \text{at} \quad y = 0 \quad \text{and} \quad y = y_0; \quad (19d)$$

$$v = \alpha \frac{dv}{dy} \quad \text{at} \quad y = 0, \quad (19e)$$

$$v = \alpha \frac{dv}{dy} \quad \text{at} \quad y = y_0; \quad (19f)$$

where  $y_0 = \frac{b}{a}$  is the aspect ratio,  $\alpha = \frac{a^*}{a}$  is the slip flow parameter and  $Bi = \frac{ah}{k_f}$  is the slip convection parameter.

### 3 Results and discussion

In this study, the mass and heat transfer of the MHD of a micropolar fluid through a rectangular duct have been solved numerically by the finite difference method with  $41 \times 41$  mesh points in both directions. The dimensionless temperature Eq. (18) and the coupled induction, velocity

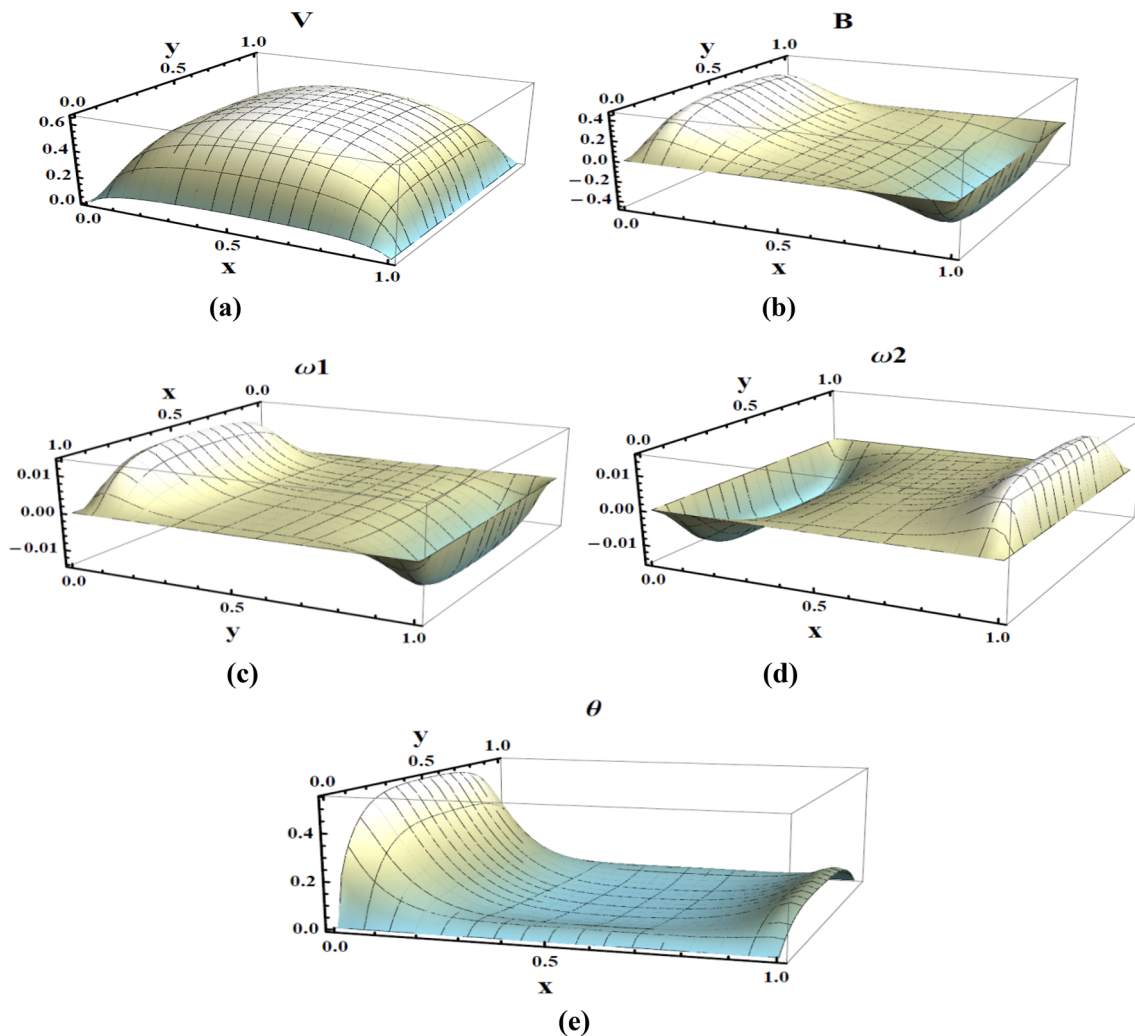


**Fig. 2** 3-Dimensional profiles of **a** velocity, **b** magnetic field, **c** microrotation in x-direction, **d** microrotation in y-direction, **e** temperature



and microrotation Eqs. (14)–(17) are solved subject to the boundary conditions (19a)–(19f). The effect of various parameters  $R_m$ ,  $R_e$ ,  $Ha$ ,  $N$ ,  $\alpha$ ,  $Bi$  and  $Br$  are presented graphically. Figure 2 show the profiles of the velocity, magnetic field, microrotation in x- and y-directions and temperature at  $R_m = 10$ ,  $R_e = 4$ ,  $Ha = 5$ ,  $N = 0.4$ ,  $\alpha = 0.1$ ,  $Bi = 1$ ,  $Br = 1$ ,  $P_l = 1$ ,  $m = 1$ ,  $l = 0.5$ ,  $A = 1$  and  $C = 0.1$ . It is clear from Fig. 2a that the maximum magnitude of the velocity at the center and decreases at the boundaries of the duct [13]. In Fig. 2b, it is observed that the maximum value of the induced

magnetic field inside the fluid between the vertical boundaries and the center of the duct, and equal zero at both of the center and the boundaries of the rectangular duct.

It is clear from Fig. 2c that the maximum values of the microrotation ( $\omega_y$ ) are situated between the horizontal boundaries and the center of the duct, and it is zero at each wall of the duct. But at the center, the value is approaching zero. Also, it is observed that the rotation in the region below the center of the duct in the positive x-direction. But above the center, it rotates in the negative x-direction,

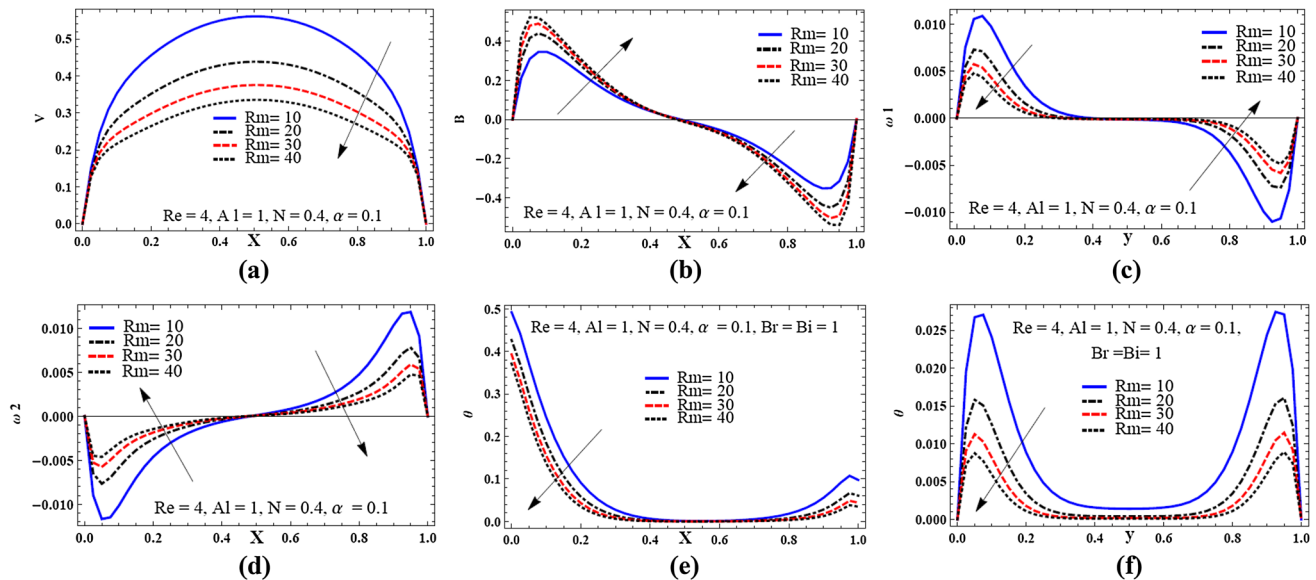


**Fig. 3** The profiles of **a** velocity, **b** magnetic field, **c** microrotation in y-direction, **d** microrotation in x-direction, **e**, **f** temperatures in x and y with various values of  $R_m$  at the centerline of the duct

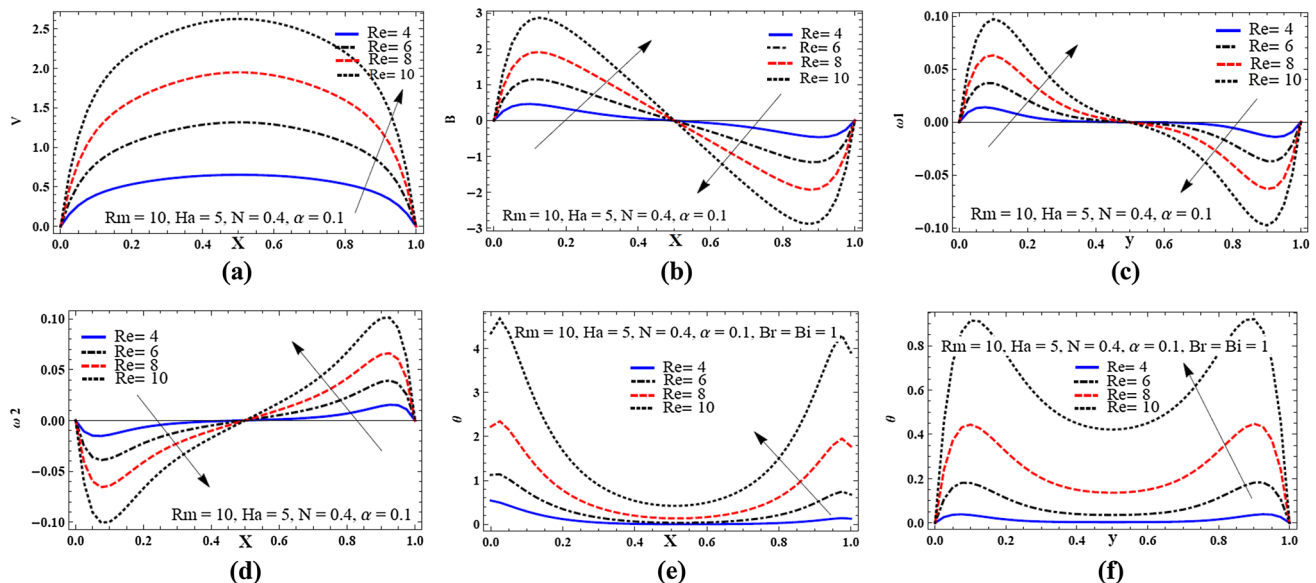


**Fig. 4** The profiles of **a** velocity, **b** magnetic field, **c** microrotation in x-direction, **d** microrotation in y-direction, **e**, **f** temperatures in x and y with various values of  $R_e$  at the centerline of the duct

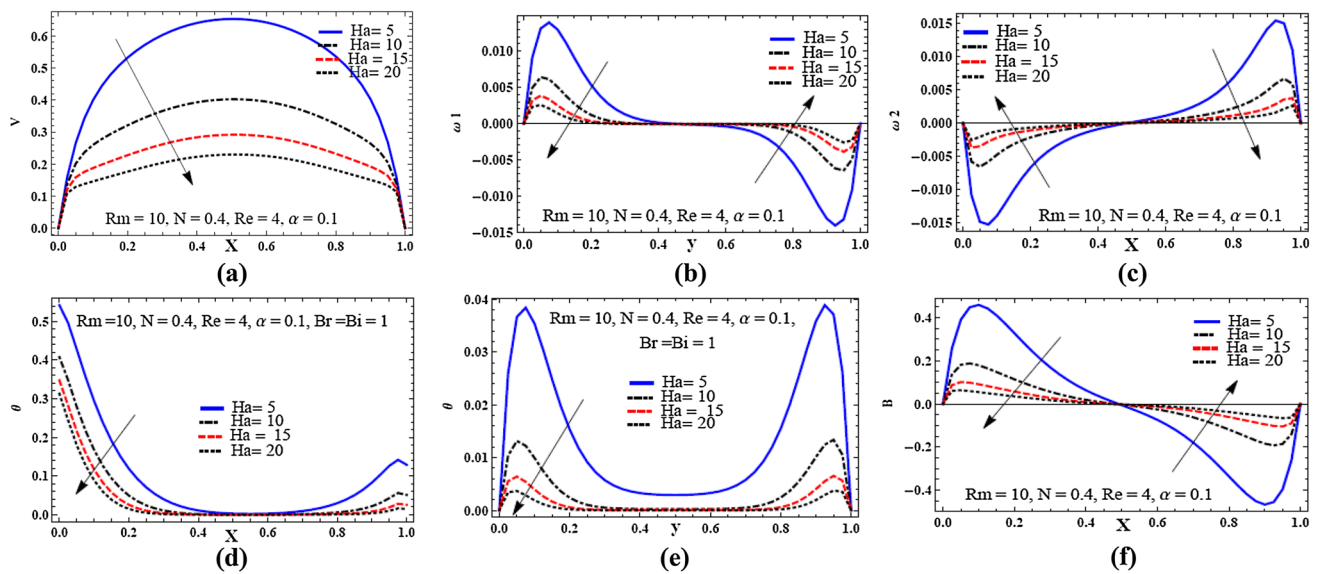


**Fig. 5** The profiles of **a** velocity, **b** Microrotation in x-direction, **c** microrotation in y-direction, **d, e** temperatures in x and y and **f** magnetic fields with various values of  $Ha$  at the centerline of the duct

while the coupling between the rotational and Newtonian viscosity is represented by the coupling number  $N$ . The vanishing to zero in the figures of microrotation means that the fluid is non-polar and the micropolarity is lost ( $k \rightarrow 0$  and  $N \rightarrow 0$ ). In Fig. 2d it is shown that the values of microrotation ( $\omega_2$ ) are maximum between the vertical walls and the center of the duct, but at the center, the value is approaching zero and tends to zero at the walls of the duct. Also, it is observed that the fluid rotates in the negative y-direction at the left region of the duct. But in the

right region, it rotates about the positive y-direction [13, 16]. Figure 2e presents the maximum magnitude of temperature along x-axis at the center of the left vertical wall and decreasing at the center of the duct, it increases by a smaller rate when approaching to the center of the right vertical wall, while the maximum value of temperature along y-axis at the center and the rate is decreased when it is near to the horizontal walls. The profiles of velocity in Fig. 3a, magnetic microrotations in Fig. 3c, d and temperatures Fig. 3e, f decrease with the increase of the magnetic

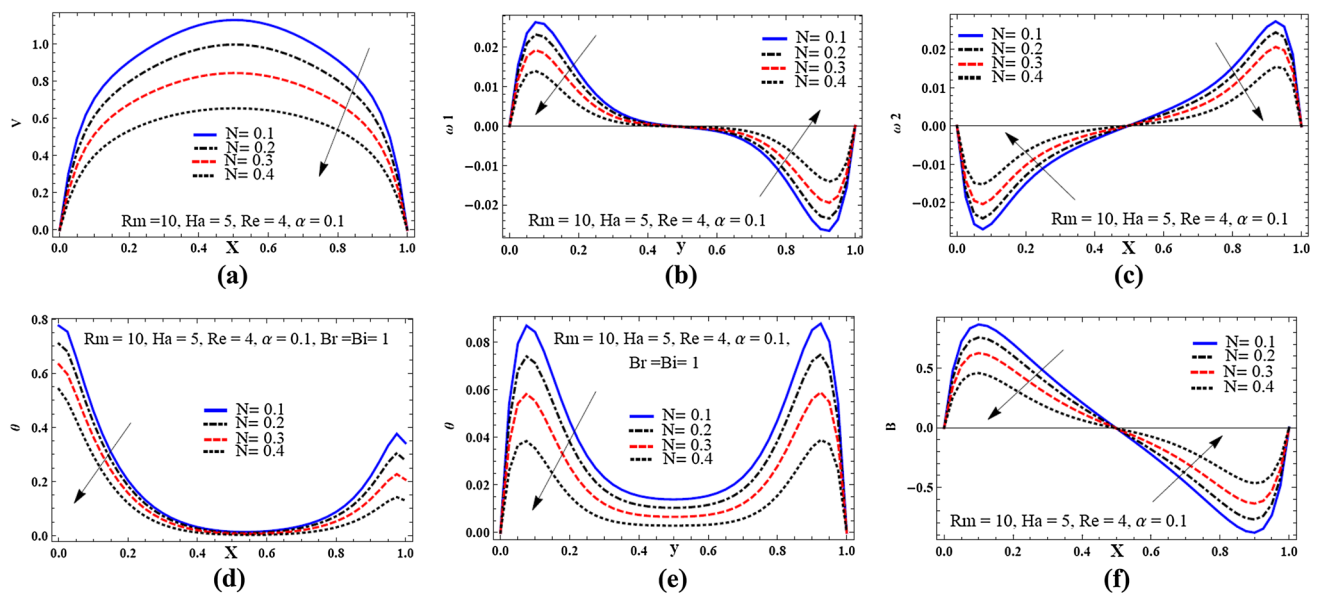


**Fig. 6** The profiles of **a** velocity, **b** Microrotation in x-direction, **c** microrotation in y-direction, **d, e** temperatures in x and y and **f** magnetic fields with various values of  $N$  at the centerline of the duct

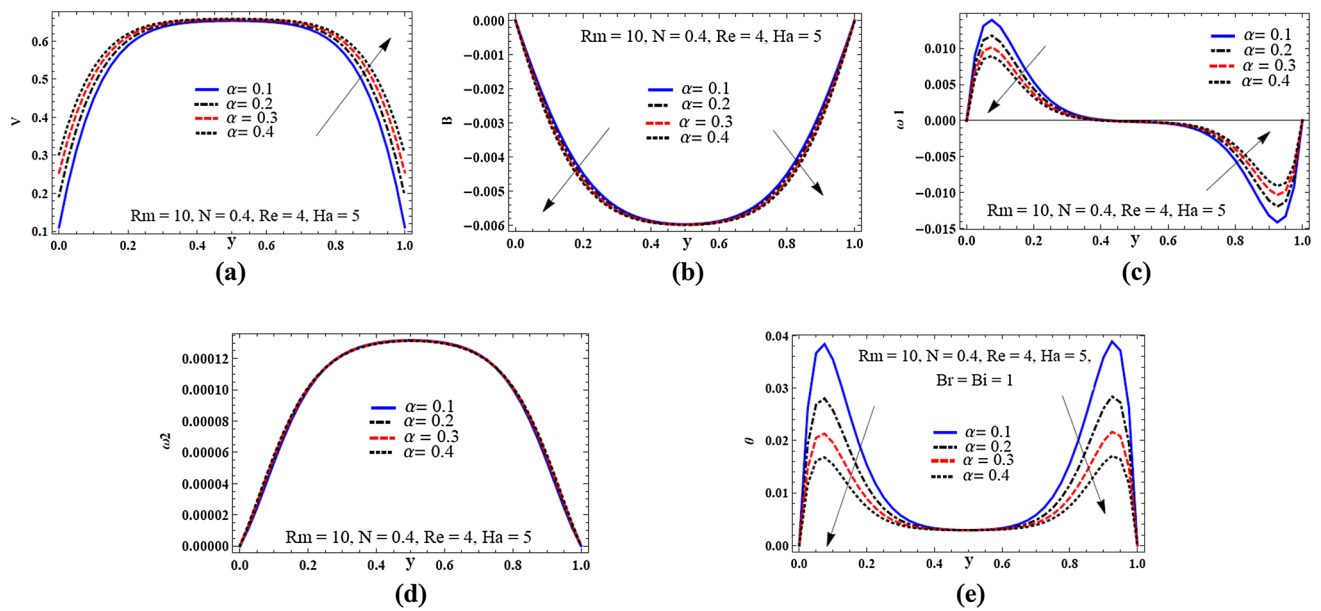


**Fig. 7** The profiles of **a** velocity, **b** magnetic field, **c** microrotation in x-direction, **d** microrotation in y-direction, **e** temperatures in y direction with various values of  $\alpha$  at the centerline of the duct

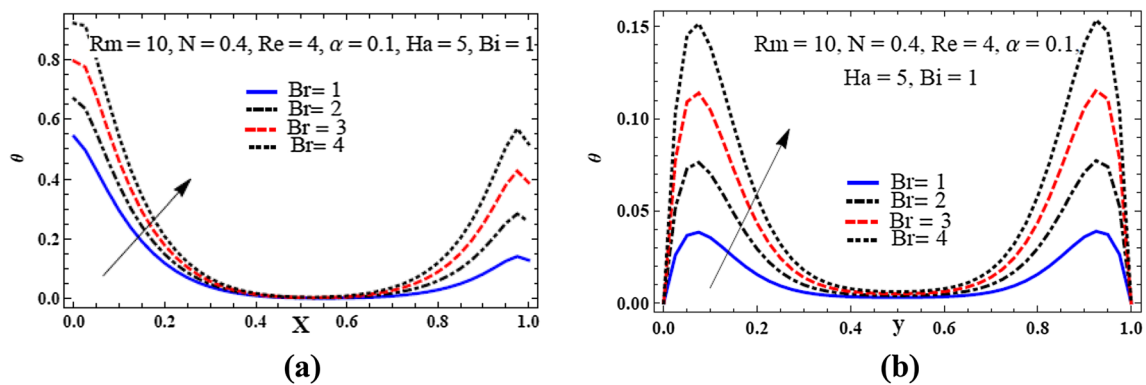


**Fig. 8** The profiles of **a** temperatures in x direction and **b** in y direction with various values of  $Br$  at the centerline of the duct

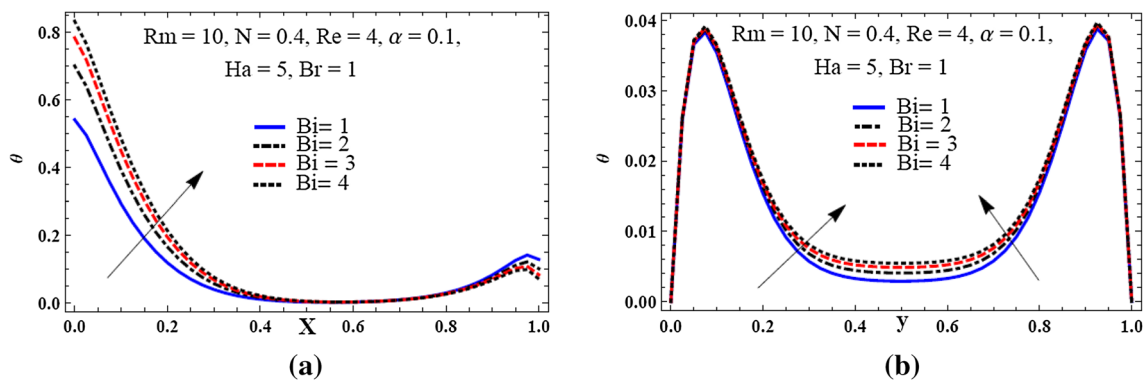


**Fig. 9** The profiles of **a** temperatures in x-direction and **b** in y-direction with various values of  $Bi$  at the centerline of the duct



Reynolds number in the entire rectangular duct, while the profiles of the induced magnetic field in Fig. 3b increase when the increase of the magnetic Reynolds number. Figure 4 show; the velocity (a), microrotations (c) and (d), induced magnetic field (b) and temperature profiles (e) and (f) are increased with increase Reynolds number.

Figure 5 show; the velocity (a), microrotations (b) and (c) decrease with the increase of the Hartmann number but, the induced magnetic field is increasing the delay the flow (decrease the velocity) compared with that occurred in [13]. Also, the induced magnetic field in Fig. 5f and temperature in Fig. 5d, e decrease with the increase of the Hartmann number. Figure 6 show; the velocity (a), microrotations (b) and (c) decrease with the increase of the coupling number but, the induced magnetic field causes to increase the delay the flow (decrease the velocity) compared with that occurred in [13]. Also, the induced magnetic field in Fig. 6f and temperature in Fig. 6d, e decrease with the increase in the coupling number. Figure 7a, d show the velocity and microrotation in y-direction are increased with the increase of the slip flow, but Fig. 7b, c, e show the induced magnetic field, microrotation in x-direction and temperature decrease with increase the slip flow.

Figure 8 present that the profile of temperature increases with increased the Brinkman number in both directions. It is clear that the Brinkman number does not exist in Eqs. (14), (15), (16) and (17) so that each of the velocity, microrotations and induced magnetic field do not enter into a discussion of Brinkman number. Figure 9 present that the profile of temperature increases with increase slip convection parameter. But does not exist in each Eqs. (19a), (19c) and (19d) so that each of the velocity, microrotations and induced magnetic field do not enter into a discussion of the slip convection parameter.

## 4 Conclusion

In this article, we presented the effect induced magnetic field into the micropolar fluid. Numerical method is used to solve the MHD equations concerning the mass and heat transfers of the steady, incompressible micropolar fluid through a rectangular duct with the effect of the induced magnetic field and slip conditions. The analysis of the micropolar fluid flow and heat transfer have been conducted by the various values of the magnetic Reynolds, Reynolds, Hartmann, coupling and Brinkman numbers, slip flow and convection parameters. Based on the obtained results, we can conclude that:

- The velocity increases with the increase Reynolds number and slip flow parameter, but decreases with the increase in magnetic Reynolds, Hartmann and cou-

pling numbers. It is not affected by the slip convection parameter and Brinkman number.

- The induced magnetic field increases with the increase of Reynolds and magnetic Reynolds numbers, but decreases with the increase of Hartmann, coupling numbers and the slip flow parameter. It is not affected by the slip convection parameter and Brinkman number.
- The microrotation in x-axis increases with the increases of Reynolds number, but decreases with the increase in magnetic Reynolds, Hartmann, coupling numbers and the slip flow parameter. It is not affected by the slip convection parameter and Brinkman number.
- The microrotation in the y-axis increase with the increases of Reynolds number and the slip flow parameter, but decreases with the increase of magnetic Reynolds, Hartmann and coupling numbers. It is not affected by the slip convection parameter and Brinkman number.
- The temperature increases with the increase of Reynolds, Brinkman numbers and the slip convection parameter, but decreases with the increase of magnetic Reynolds, Hartmann, coupling numbers and the slip flow parameter.

**Acknowledgements** The authors are grateful to the anonymous referee for his suggestions, which have greatly improved the presentation of the paper.

**Authors' contribution** The author has made an equal contribution. The author read and approved the final manuscript.

## Compliance with ethical standards

**Conflict of interest** The authors declare that they have no competing interests.

## References

1. Eringen AC (1964) Simple microfluids. *Int J Eng Sci* 2(2):205–217
2. Eringen AC (1966) Theory of micropolar fluids. *J Math Mech* 16:1–18
3. Eringen AC (1972) Theory of thermomicrofluids. *J Math Anal Appl* 38(2):480–496
4. Subba R, Gorla R, Nakamura S (1995) Mixed convection of a micropolar fluid from a rotating cone. *Int J Heat Fluid Flow* 16(1):69–73
5. Vantighem S, Knaepen B (2011) Numerical simulation of magnetohydrodynamic flow in a toroidal duct of square cross-section. *Int J Heat Fluid Flow* 32(6):1120–1128
6. Chou F, Hwang G (1987) Vorticity-velocity method for the Graetz problem and the effect of natural convection in a horizontal rectangular channel with uniform wall heat flux. *J Heat Transf* 109(3):704–710

7. Aung W, Worku G (1987) Mixed convection in ducts with asymmetric wall heat fluxes. *J Heat Transf* 109(4):947–951
8. Mahaney H, Incropera F, Ramadhyani S (1987) Development of laminar mixed convection flow in a horizontal rectangular duct with uniform bottom heating. *Numer Heat Transf* 12(2):137–155
9. Huang C-C, Yan W-M, Jang J-H (2005) Laminar mixed convection heat and mass transfer in vertical rectangular ducts with film evaporation and condensation. *Int J Heat Mass Transf* 48(9):1772–1784
10. Sayed-Ahmed ME, Attia HA (2005) The effect of Hall current on magnetohydrodynamic flow and heat transfer for Bingham fluids in a rectangular duct. *Can J Phys* 83(6):637–651
11. Ramakrishna K, Rubin S, Khosla P (1982) Laminar natural convection along vertical square ducts. *Numer Heat Transf* 5(1):59–79
12. Abd-Alla A, Yahya G, Mahmoud S, Alosaimi H (2012) Effect of the rotation, magnetic field and initial stress on peristaltic motion of micropolar fluid. *Meccanica* 47(6):1455–1465
13. Srinivasacharya D, Shiferaw M (2008) MHD flow of micropolar fluid in a rectangular duct with hall and ion slip effects. *J Braz Soc Mech Sci Eng* 30(4):313–318
14. Pandey S, Chaube M (2011) Peristaltic flow of a micropolar fluid through a porous medium in the presence of an external magnetic field. *Commun Nonlinear Sci Numer Simul* 16(9):3591–3601
15. Reddy GJ, Kethireddy B, Beg OA (2018) Flow visualization using heat lines for unsteady radiative hydromagnetic micropolar convection from a vertical slender hollow cylinder. *Int J Mech Sci* 140:493–505
16. Ayano MS, Sikwila ST, Shateyi S (2018) MHD mixed convection micropolar fluid flow through a rectangular duct. *Math Probl Eng* 2018
17. Miroschnichenko IV, Sheremet MA, Pop I, Ishak A (2017) Convective heat transfer of micropolar fluid in a horizontal wavy channel under the local heating. *Int J Mech Sci* 128:541–549
18. Shit G, Roy M (2015) Effect of slip velocity on peristaltic transport of a magneto-micropolar fluid through a porous non-uniform channel. *Int J Appl Comput Math* 1(1):121–141
19. Bhattacharyya K, Layek G, Seth G (2014) Soret and Dufour effects on convective heat and mass transfer in stagnation-point flow towards a shrinking surface. *Phys Scr* 89(9):095203
20. Sheremet MA, Pop I, Ishak A (2017) Time-dependent natural convection of micropolar fluid in a wavy triangular cavity. *Int J Heat Mass Transf* 105:610–622
21. Gupta D, Kumar L, Bég OA, Singh B (2018) Finite element analysis of MHD flow of micropolar fluid over a shrinking sheet with a convective surface boundary condition. *J Eng Thermophys* 27(2):202–220
22. Srinivasacharya D, Himabindu K (2017) Analysis of entropy generation due to micropolar fluid flow in a rectangular duct subjected to slip and convective boundary conditions. *J Heat Transf* 139(7):072003

**Publisher's Note** Springer Nature remains neutral with regard to jurisdictional claims in published maps and institutional affiliations.